

Enhanced Anticancer Activity of PF-04691502, a Dual PI3K/mTOR Inhibitor, in Combination With VEGF siRNA Against Non–small-cell Lung Cancer

Laura Espana-Serrano¹ and Mahavir B Chougule^{1–5}

Lung cancer is the leading cause of cancer deaths in both men and women in the United States accounting for about 27% of all cancer deaths. In our effort to develop newer therapy for lung cancer, we evaluated the combinatory antitumor effect of siRNA targeting VEGF and the PI3K/mTOR dual inhibitor PF-04691502. We analyzed the anticancer effect of siRNA VEGF and PF-04691502 combination on proliferation, colony formation and migration of A549 and H460 lung cancer cells. Additionally, we assessed the combination treatment antiangiogenic effect on human umbilical vein endothelial cells. Here, we show for the first time that the antiangiogenic siRNA VEGF potentiates the PF-04691502 anticancer activity against non–small-cell lung cancer. We observed a significant ($P < 0.05$) decrease in cell viability, colony formation, and migration for the combination comparing with the single drug treatment. We also showed a significant ($P < 0.05$) enhanced effect of the combination treatment inhibiting angiogenesis progression and tube formation organization compared to the single drug treatment groups. Our findings demonstrated an enhanced synergistic anticancer effect of siRNA VEGF and PF-04691502 combination therapy by targeting two main pathways involved in lung cancer cell survival and angiogenesis which will be useful for future preclinical studies and potentially for lung cancer patient management.

Molecular Therapy—Nucleic Acids (2016) 5, e384; doi:10.1038/mtna.2016.90; published online 15 November 2016

Subject Category: Therapeutic proof of concept

Introduction

Lung cancer is the leading cause of cancer-related mortality among both men and women, with an estimated 158,040 deaths in 2015 in the United States.¹ Non–small-cell lung cancer (NSCLC) is the most prevalent type of lung cancer, with more than 85% of the cases.¹ Majority of patients newly diagnosed with NSCLC present with locally advanced or metastatic disease beyond the scope of surgical cure.² As a result, systemic chemotherapy continues to be the mainstay of treatment to improve the survival and quality of life of patients.³ In the last years, newer drugs that specifically target molecular pathways in NSCLC have been FDA approved showing promising results for the treatment of lung cancer.⁴ Despite recent advances, response rates in NSCLC remain <50% and the 5-year survival rate for stage IV disease is about 1%.¹ To address this problem, attention has been focused on finding novel combinations of anticancer agents to achieve enhanced efficacy with decreased side effects.

Lung cancer has wide molecular heterogeneity and therefore, warrants the targeting of multiple pathways for effective therapy.⁵ Tumor angiogenesis is a hallmark of cancer.⁶ Currently, newer approaches using antiangiogenic agents in combination with other anticancer drugs have generated

clinical interest.⁷ Vascular endothelial growth factor (VEGF) is a major angiogenesis inducer that mediates numerous changes within the tumor vasculature, including endothelial cell proliferation, vascular permeability, migration, invasion, and survival.⁸ VEGF activates the VEGF receptor (VEGFR) inducing the phosphorylation of several proteins and the activation of different signaling pathways (Figure 1a). A consistent increase in VEGF expression has been observed in solid tumors of different origins.⁹ In NSCLC, the VEGF overexpression (61 to 92% of the tumors) is associated with tumor growth, metastasis, and poor survival.^{10,11} Anti-VEGF treatment has been proven to have a survival benefit as anticancer therapy to prevent NSCLC progression¹² but clinical trials failed to demonstrate a meaningful clinical benefit to patients. The use of VEGF antibodies has been limited due to poor efficacy and adverse effects.^{13,14} Therapeutic antibodies have some functional limitations as inadequate pharmacokinetics, poor oral bioavailability and tissue accessibility, incomplete absorption, nonlinear distribution and elimination, and impaired interactions with the immune system.¹⁵ Small interference RNA (siRNA) represents an emerging therapeutic tool for cancer therapy and may overcome some of these limitations.¹⁶ The advantages of siRNA are its high degree of efficacy and safety. siRNA can potentially inhibit gene

¹Translational Drug Delivery Research (TransDDR) Laboratory, Department of Pharmaceutical Sciences, Daniel K. Inouye College of Pharmacy, University of Hawaii at Hilo, Hilo, Hawaii, USA; ² Translational Drug and Gene Delivery Research (TransDGDR) Laboratory, Department of Pharmaceutics and Drug Delivery, School of Pharmacy, University of Mississippi, Oxford, MS; ³ Pii Center for Pharmaceutical Technology, Research Institute of Pharmaceutical Sciences, University of Mississippi, Oxford, MS; ⁴ National Center for Natural Products Research, Research Institute of Pharmaceutical Sciences, University of Mississippi, Oxford, MS; ⁵ Natural Products and Experimental Therapeutics Program, University of Hawaii Cancer Center, Honolulu, Hawaii, USA. Correspondence: Mahavir B. Chougule, Department of Pharmaceutics and Drug Delivery, School of Pharmacy, Faser Hall, The University of Mississippi, Oxford MI 38677, USA. E-mail: chougule@olemiss.edu; mahavirchougule@gmail.com

Keywords: combination therapy; non–small-cell lung cancer; mTOR; PI3K; PF-04691502; siRNA; VEGF

Received 16 February 2016; accepted 8 September 2016; published online 15 November 2016. doi:10.1038/mtna.2016.90

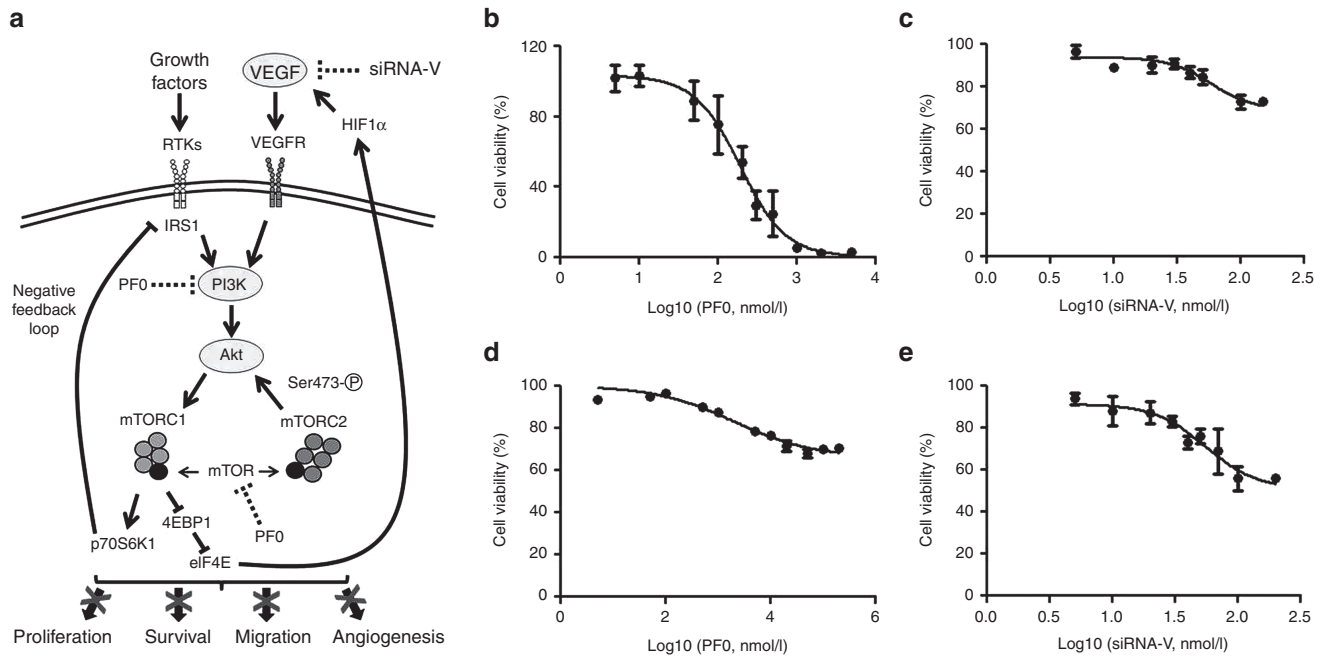


Figure 1 Dose response cytotoxicity of PF0 and siRNA-V against NSCLC cell lines. (a) Schematic representation of VEGF and PI3K/Akt/mTOR interconnected signaling pathways and the inhibition sites of siRNA-V and PF0. Growth factors binding to their cognate RTKs activate the PI3K pathway. VEGFR activation by its ligand VEGF leads to PI3K activation and Akt phosphorylation. The mTORC2 complex activates Akt phosphorylation. Akt activates mTORC1 complex. PI3K/Akt/mTOR pathway can increase VEGF secretion via eIF4E-mediated HIF-1 α activation. siRNA-V and PF0 effect leads to inhibition of cell proliferation, survival, migration and angiogenesis. (b) *In vitro* cytotoxicity profile of A549 cells after 72 hours treatment with PF0 (5 to 5,000 nmol/l), (c) A549 cells after 72 hours treatment with siRNA-V (5 to 150 nmol/l), (d) H460 cells after 72 hours treatment with PF0 (5 nmol/l to 200 μ mol/l), and (e) H460 cells after 72 hours treatment with siRNA-V (5 to 200 nmol/l). Cells were treated and cytotoxicity was determined using the resazurin dye assay as described in Materials and Methods. Values represent mean \pm standard deviation of three independent experiments for each treatment group. Dose-dependent inhibition of cell proliferation was noted.

expression with high sequence selectivity, decreasing the protein expression instead of only sequestering the protein. Opko Health produced the first siRNA therapeutic to reach a phase 3 clinical trial, bevasiranib, targeting VEGF.¹⁷ VEGF-siRNA (siRNA-V) has demonstrated promising *in vitro* and *in vivo* antitumor activity,^{18,19} and will be an efficient alternative for lung cancer treatment.

The phosphatidylinositol 3-kinase (PI3K)/mammalian target of rapamycin (mTOR) signaling pathway plays a central role in regulating cell growth, proliferation, survival, angiogenesis, metabolism, and motility.²⁰ The PI3K pathway has been extensively studied in relation to a variety of cancers in recent years.²¹ Deregulation of PI3K signaling cascade is known to be involved in lung tumorigenesis and it has been associated with high grade tumors and more advanced disease in NSCLC.²² Several mechanisms of crosstalk have been reported between VEGF and PI3K pathways.²³ Activation of the PI3K/Akt/mTOR cascade in tumor cells can increase VEGF secretion by both HIF1 α -dependent and -independent mechanisms.²⁴ Several mTOR inhibitors have been FDA approved in recent years and some PI3K inhibitors are already in phase 3 clinical trials. Emerging clinical data show limited single-agent activity of inhibitors targeting PI3K or mTOR at tolerated doses. PI3K/mTOR dual inhibitors target the active sites of both proteins inhibiting the pathway both upstream and downstream of Akt, overcoming the

mTORC1–p70S6K–IRS1 negative feedback loop, and blocking PI3K-independent mTOR activation^{21,25} (Figure 1a). Dual PI3K/mTOR inhibitors are being tested in preclinical and early-stage clinical studies and have shown promising results in terms of safety and efficacy.^{26,27} Some of these agents are beginning to enter phase 2 clinical trials in a variety of diseases.²² The dual inhibitor PF-04691502 (PF0) potentially inhibits PI3K and mTOR in biochemical assays.²⁸

Considering the crucial role of VEGF and PI3K/mTOR pathways in lung cancer and the crosstalk connection between them, we hypothesize that the combination of siRNA-V and PF0 will have an enhanced anticancer effect by reducing tumor cell growth, survival, and migration comparing with single-agent treatment. To the best of our knowledge, we demonstrated for the first time that the anticancer activity of PF0 was enhanced in a synergistic manner in combination with VEGF siRNA against lung cancer. We have adopted a unique approach by combining siRNA-V treatment with PF0 to target three important proteins, VEGF, PI3K, and mTOR involved in NSCLC to enhance the therapeutic outcome. PF0 and siRNA-V synergistic combination may improve therapeutically relevant selectivity and enable improved control of complex biological systems offering the possibility of dose reduction and decrease adverse side effects. The results of this study may pave the way toward new therapies for lung cancer.

Results

Dose response cytotoxicity analysis

The *in vitro* cytotoxicity of PF0 (5 to 5,000 nmol/l) or siRNA-V (5 to 150 nmol/l) was evaluated against A549 cells after 24, 48, and 72 hours treatment (Figure 1b,c and Supplementary Figure S1). PF0 and siRNA-V cytotoxicity was found to be dose and time dependent. PF0 IC₅₀ values in A549 cells were 209.77±34.23 nmol/l; 151.45±35.34 nmol/l; 191.60±39.66 nmol/l after 24, 48, and 72 hours treatment respectively (Figure 1b and Supplementary Figure S1a). siRNA-V has limited effect on A549 cell viability with a maximum decrease of 27% after 72 hours 100 nmol/l siRNA-V treatment (Figure 1c). IC₅₀ values for siRNA-V in A549 cells were 19.04±14.71 nmol/l; 28.49±14.22 nmol/l; 58.89±78.10 nmol/l after 24, 48, and 72 hours of treatment (Figure 1c and Supplementary Figure S1b). In H460 cells, PF0 (5 nmol/l to 200 μmol/l) or siRNA-V (5 to 200 nmol/l) cytotoxicity was also found to be dose and time dependent (Figure 1d,e and Supplementary Figure S2). IC₅₀ values for PF0 in H460 cells were 1,965.5±131.7 nmol/l; 1,080.1±307.1 nmol/l; 936.7±174.6 nmol/l after 24, 48, and 72 hours of treatment respectively (Figure 1d and Supplementary Figure S2a). Cell viability was decreased a maximum of 42% after 72 hours of 100 nmol/l siRNA-V treatment (Figure 1e). IC₅₀ values for siRNA-V were 26.19±9.18 nmol/l; 37.78±3.71 nmol/l; 40.79±13.73 nmol/l after 24, 48, and 72 hours of treatment against H460 cells (Figure 1e and Supplementary Figure S2b).

siRNA-V and PF0 combination cytotoxicity assays

We evaluated the combination cytotoxicity effect of siRNA-V (50 nmol/l) and PF0 (5 to 500 nmol/l for A549, and 10 to 5,000 nmol/l for H460 cells) compared to the single agents (Figure 2). After 24, 48, and 72 hours treatment with siRNA-V and PF0, we observed a significant ($P < 0.05$) decrease in relative cell viability for the combination compared to single-agent treatments (Figure 2a,b). The combination cytotoxicity assays demonstrated that siRNA-V potentiates the anticancer activity of PF0 against A549 and H460 cells.

VEGF silencing effect analysis by quantitative real-time PCR

We analyzed the effect of siRNA-V and PF0 combination and single agents on VEGF mRNA expression in A549 and H460 cells. Cells were treated with siRNA-V (50 nmol/l) and PF0 (200 nmol/l for A549 and 2,000 nmol/l for H460) combination and single agents for 48 hours. PF0 and siRNA-V concentrations were selected based on the previous single-agent cytotoxicity results. VEGF and glyceraldehyde-3-phosphate dehydrogenase (GAPDH) mRNA levels were evaluated using a quantitative real-time polymerase chain reaction (PCR). In A549 cells, the siRNA-V treatment showed a significant ($P < 0.05$) decrease of 62.58±16.60% in VEGF gene expression compared to control (Figure 3a). siRNA-V and PF0 combination treatment showed a significantly ($P < 0.01$) decreased VEGF expression of 75.06±13.21% compared to control. In H460 cells, we observed a significant ($P < 0.001$) decrease in the relative VEGF mRNA expression after siRNA-V transfection by 92.22±3.10% as well as after the combination treatment 69.59±7.71% compared to control cells (Figure 3b).

Secreted VEGF protein expression analysis by ELISA

Human VEGF protein concentration was measured by Enzyme-linked immunosorbent assay (ELISA) in A549 and H460 cells after 24, 48, and 72 hours siRNA-V and PF0 combination and single-agent treatments. In A549 and H460 control cells, the VEGF levels increased in a time-dependent manner (Figure 3c,d). ELISA showed significantly ($P < 0.05$) decreased VEGF protein levels after exposure to PF0 in both A549 (200 nmol/l) and H460 (2,000 nmol/l) cells after 24, 48, and 72 hours comparing with control cells. ELISA showed significant ($P < 0.01$) differences in VEGF protein expression after siRNA-V treatment (50 nmol/l) compared with control samples for A549 and H460 cells after 24, 48, and 72 hours treatment (Figure 3c,d). The combination treatment resulted in a significantly ($P < 0.05$) stronger reduction in the VEGF protein secretion when compared with single-agent treatments in both A549 and H460 cells, with almost undetectable VEGF levels observed after 24, 48, and 72 hours (Figure 3c,d).

Western blot analysis of PI3K and mTOR downstream effectors

Western blot analysis was used to examine whether the PF0 treatment and the combination with siRNA-V could effectively inhibit the phosphorylation of target proteins in the PI3K and mTOR pathway. Akt and p70S6K phosphorylation was significantly ($P < 0.05$) suppressed by PF0 (at 200 nmol/l in A549 and 2,000 nmol/l concentration in H460 cells) as single drug or in combination with 50 nmol/l siRNA-V in both NSCLC cell lines and after 24, 48, and 72 hours treatment (Figure 3e,f and Supplementary Figures S3 and S4).

Inhibition of anchorage-dependent colony formation

Colony formation assay was used to investigate long-term effect of PF0 and siRNA-V on proliferation of A549 and H460 cells. We treated cells with siRNA-V (50 nmol/l) and PF0 (200 nmol/l for A549 and 2,000 nmol/l for H460) combination and single agents (Figure 4a-d). A549 relative colony-forming ability was reduced after PF0 treatment to 77.50±3.79% and after exposure to siRNA-V to 62.10±12.12% as compared with control (Figure 4a,c). The reduction was more remarkable after PF0 was combined with siRNA-V showing a significant ($P < 0.05$) decrease in colony formation to a 29.83±8.11% as compared with control. For A549 cells, the combination resulted in a significant ($P < 0.05$) colony formation reduction when compared with PF0 treatment (Figure 4c). The relative colony-forming ability of H460 cells was reduced after PF0 treatment to 61.86±20.48% and after siRNA-V treatment to 73.21±1.97% as compared with controls (Figure 4b,d). PF0 and siRNA-V combination showed a significant ($P < 0.05$) decrease in relative colony formation to 7.97±9.20% as compared with control groups. The combination resulted in a significant ($P < 0.01$) decrease in the H460 colony formation when compared with single-agent treatment (Figure 4d).

Inhibition of cell migration

The effect of siRNA-V and PF0 in A549 and H460 cell migration was investigated using a monolayer *in vitro* wound healing assay. The wound widths were imaged and quantified

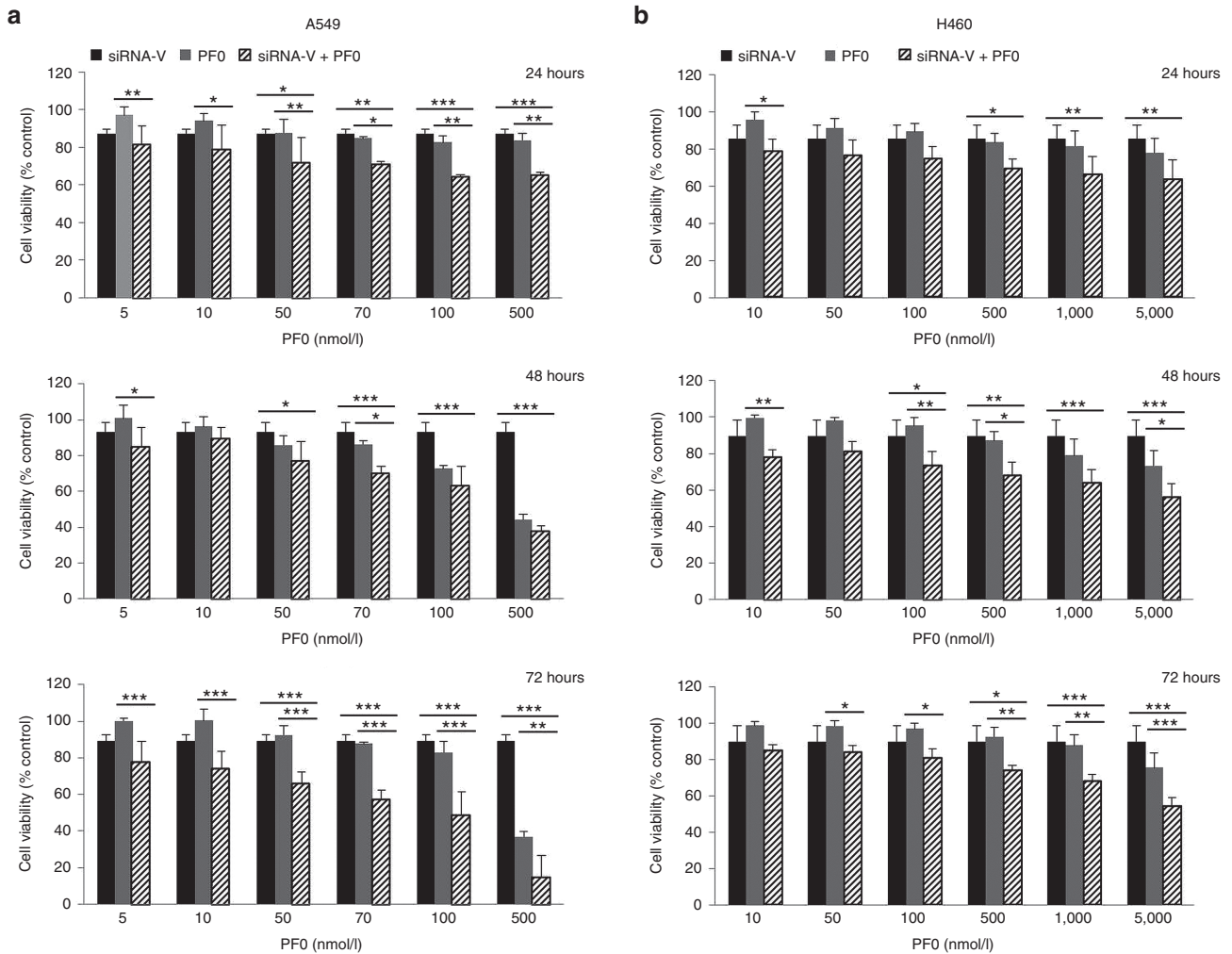


Figure 2 siRNA-V and PF0 combination cytotoxicity assays. Relative effect of siRNA-V and PF0 combination against (a) A549 and (b) H460 cells after 24, 48, and 72 hours treatment with 50 nmol/l siRNA-V and varying concentrations of PF0 (5 to 500 nmol/l for A549 cells and 10 to 5,000 nmol/l for H460 cells) single agents and in combination. Values represent the mean \pm standard deviation of three independent experiments. Asterisks indicate statistical significance (* $P < 0.05$, ** $P < 0.01$, *** $P < 0.001$).

at different time points (Figure 5a–d). We observed a significant ($P < 0.05$) effect of 50 nmol/l siRNA-V on A549 cell migration as compared with scrambled siRNA-treated cells (Figure 5c). A549 and H460 cells also showed significant ($P < 0.05$) differences between PF0 (200 nmol/l for A549 and 2,000 nmol/l for H460) treated and nontreated cells (Figure 5c,d). Furthermore, combination treatment significantly ($P < 0.05$) decreased A549 and H460 cell migration compared to control cells (Figure 5c,d). A549 cells showed that after 16 hours of 50 nmol/l siRNA-V and 200 nmol/l PF0 treatment wound closure was $18.48 \pm 1.60\%$ comparing with $47.24 \pm 2.09\%$ of the control treated cells. After 40 hours treatment, A549 control cells migrated completely closing the wound while closure was reduced to $51.28 \pm 0.96\%$ for combination treated cells (Figure 5a,c). After 16 hours combination treatment, H460 wound closure was inhibited to $14.65 \pm 2.53\%$ comparing with $26.86 \pm 1.76\%$ of the control. Wound closure was $25.01 \pm 3.06\%$ after 40 hours combination treatment compared to $51.42 \pm 1.47\%$ of

the control, and $45.41 \pm 6.54\%$ after 64 hours compared to $74.02 \pm 3.09\%$ of the control (Figure 5b,d). A549 and H460 cell migration was significantly ($P < 0.05$) reduced after combination treatment compared to single agents (Figure 5).

Antiangiogenic effect analysis via inhibition of tube formation

Antiangiogenic effect of 50 nmol/l siRNA-V and 100 nmol/l PF0 was analyzed using tube formation assays of human umbilical vein endothelial cells (HUVEC) (Figure 6a–e). siRNA-V 6 hours treatment showed a significant ($P < 0.01$) decrease in tube meshes area to $57.24 \pm 3.22\%$ (Figure 6c) and segments length to $74.34 \pm 1.32\%$ (Figure 6e) compared to control. PF0 treatment showed poor organization of HUVEC tube-like structures and a nonsignificant ($P < 0.05$) decrease in segments length ($75.63 \pm 13.71\%$) compared to control (Figure 6e). The combination treatment showed an enhanced effect decreasing progression of angiogenesis with

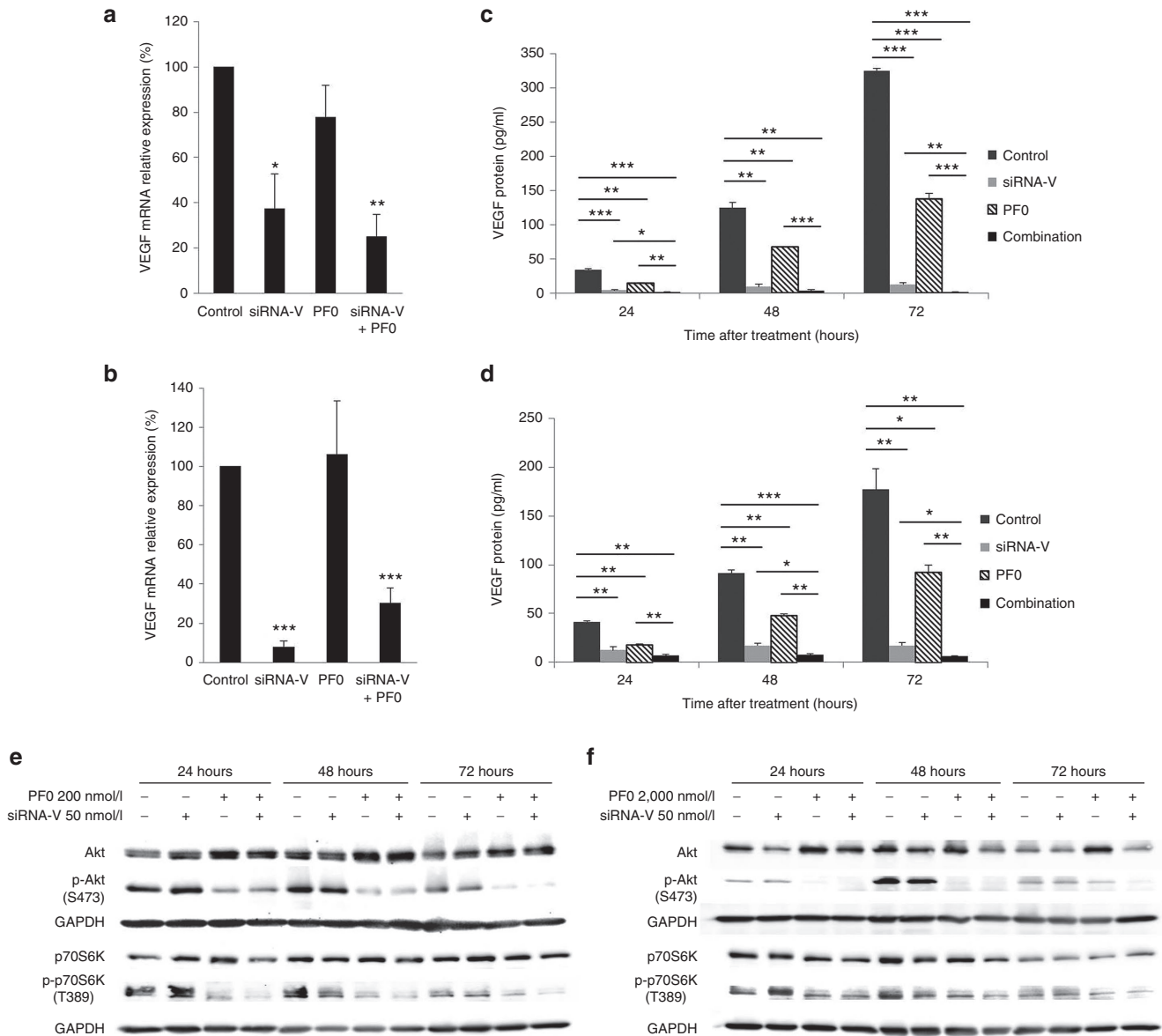


Figure 3 Relative mRNA and protein expression of VEGF, and PI3K/ mTOR downstream effectors. Relative VEGF mRNA expression levels in (a) A549 and (b) H460 cells were determined by RT-PCR after 48 hours siRNA-V and PF0 single-agent and combination treatments. The values are expressed relative to the scramble siRNA control treated cells. The target gene *VEGF* was normalized to the average of the control gene *GAPDH*. Secreted human VEGF protein levels were measured in (c) A549 and (d) H460 cells using an enzyme-linked immunosorbent assay after 24, 48, and 72 hours treatment with siRNA-V and PF0 single-agent and combination and VEGF silencing effect was detected. Values were given as mean value \pm standard deviation of three independent experiments. Asterisks indicate statistical significance as determined by Student's *t*-test (* $P < 0.05$, ** $P < 0.01$, *** $P < 0.001$). Relative protein expression levels of phospho-Akt (p-Akt), Akt, phospho-p70S6K (p-p70S6K), and p70S6K in (e) A549 and (f) H460 cells were determined by western blot analysis. A549 and H460 cells were transiently transfected with 50 nmol/l of siRNA-V and/or were treated with PF0 (200 nmol/l in A549 cells, 2,000 nmol/l in H460 cells) using the corresponding controls. After 24, 48, and 72 hours of incubation p-Akt, Akt, p-p70S6K, and p70S6K were detected using appropriate antibodies. Twenty micrograms of whole-cell lysate were used and GAPDH served as a protein loading control. All results represent three independent experiments.

a significant ($P < 0.05$) decrease in master segments length to $53.34 \pm 3.03\%$, meshes area to $14.72 \pm 17.82\%$, branches to $49.73 \pm 4.54\%$ and segments formed to $52.01 \pm 6.73\%$ compared with control (Figure 6b–e). The combination effect was increased compared to PF0 showing a significant ($P < 0.05$) decrease of the master segment length from 91.02 ± 10.99 to $53.34 \pm 3.03\%$ (Figure 6b) and meshes area from 82.64 ± 9.13 to $14.72 \pm 17.82\%$ (Figure 6c). The

combination treatment also showed a significant ($P < 0.05$) decrease in total segment length ($52.01 \pm 6.73\%$) compared to siRNA-V ($74.34 \pm 1.32\%$) (Figure 6e).

Combination index analysis, normalized isobologram, and Fa-CI plot

To test whether the combination treatment with PF0 and siRNA-V induces synergistic cell death in NSCLC, we analyzed

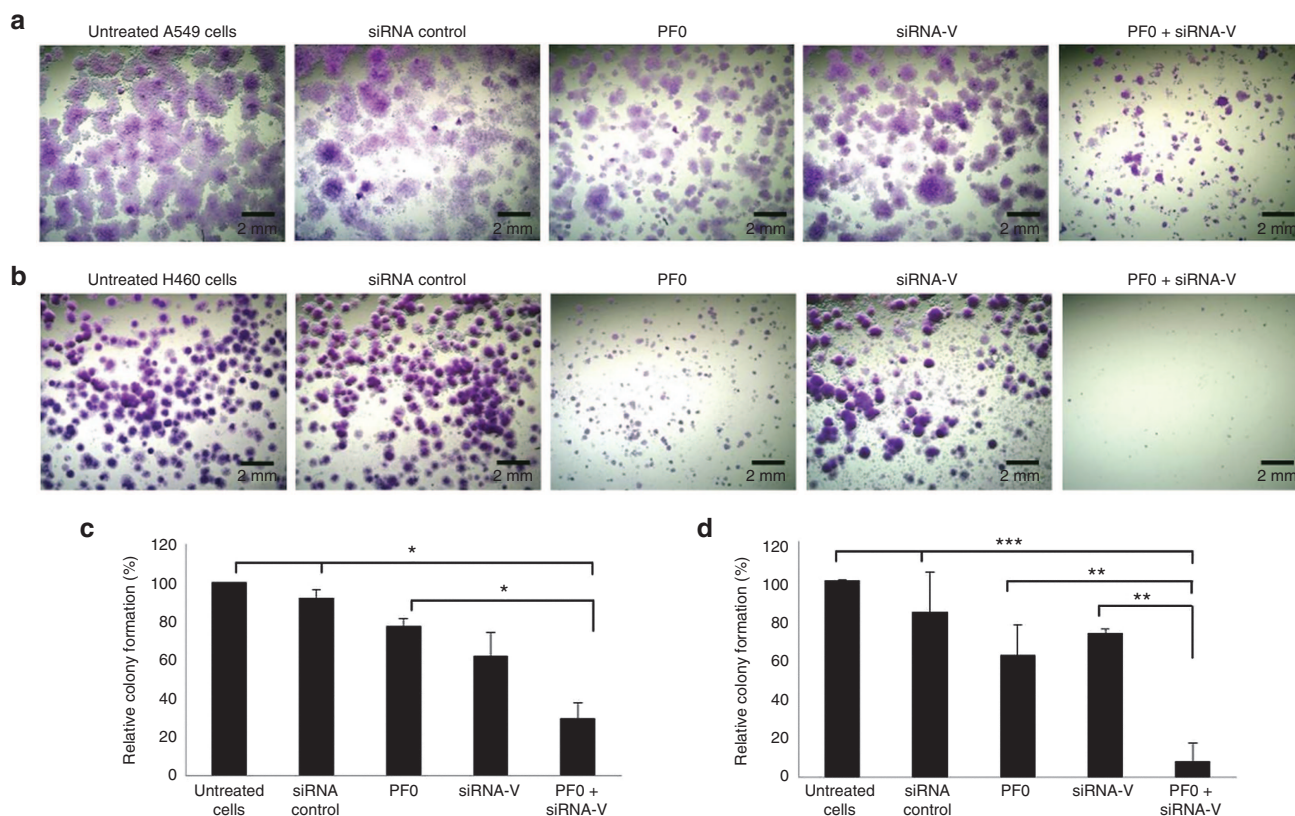


Figure 4 Inhibition of colony formation by siRNA-V and PF0. Representative images of the anchorage-dependent colony formation assay in (a) A549 and (b) H460 cells after siRNA-V (50 nmol/l) and PF0 (200 nmol/l for A549, 2,000 nmol/l for H460) single-agent and combination treatment. Quantification of (c) A549 and (d) H460 relative colony formation (%) using ImageJ 1.49 colony counter plugin. Values were given as mean value \pm standard deviation of three independent experiments. Asterisks indicate statistical significance (* $P < 0.05$, ** $P < 0.01$, *** $P < 0.001$).

drug–drug interactions using normalized isobologram for non-constant ratio combination design and combination index (CI) analysis. We treated A549 and H460 cells with a fixed dose of siRNA-V (0.1, 0.2, and 0.3 IC_{50} equivalents) and varying concentrations of PF0 (5 nmol/l to 5 μ mol/l for A549, and 5 nmol/l to 100 μ mol/l for H460 cells) to evaluate the combination cytotoxicity effect compared to the single agents after 72 hours treatment. We calculated the CI values at 0.5 fraction affected (F_a), indicating 50% of cells inhibited after drug exposure (Table 1), and generated normalized isobolograms (Figure 7a,b) illustrating the observed synergy. In A549 cells PF0 and siRNA-V combination revealed a moderate synergism at 6 and 12 nmol/l siRNA-V concentration, and slight synergism at 18 nmol/l, with CI values between 0.62 and 0.88 (Figure 7a, Table 1). In H460 cells, PF0 and siRNA-V showed moderate synergism at 4 nmol/l siRNA-V concentration, synergism at 6 nmol/l, and slight synergism at 12 nmol/l, with CI values between 0.51 and 0.81 (Figure 7b, Table 1). F_a versus CI plots were generated for A549 and H460 cells (Figure 7c,d) showing the observed synergism at $F_a = 0.5$, with CI values < 1 . The combination cytotoxicity assays demonstrated that siRNA-V synergistically potentiates the anticancer activity of PF0 against A549 and H460 cells.

Discussion

Poor clinical outcome of the current therapies for lung cancer has prompted the need for new strategies. In the last years, newer biological agents specifically targeting molecular pathways in NSCLC have been FDA approved.^{4,29} However, the efficacy and safety of these treatments are limited and the 5-year survival rate is still only 15%.¹ Our laboratory is investigating newer combination therapies for lung cancer treatment.^{30–32} One of the promising treatments for lung cancer are antiangiogenic agents that inhibit tumor growth, proliferation, and metastasis.^{7,12} Several signaling molecules governing angiogenesis are of interest, including VEGF and PI3K.³³ The overexpression of VEGF correlates with tumor growth, metastasis,^{10,34} and poor prognosis.^{11,35} Treatment with anti-VEGF antibodies has been proven to have a survival benefit to prevent NSCLC progression but their use have been limited due to poor efficacy and adverse effects.^{13,14} Therapeutic antibodies, including Bevacizumab, have some functional limitations.¹⁵ siRNA represents an emerging tool that is expected to overcome some of these limitations.³⁶ siRNA can potently inhibit gene expression with high sequence selectivity decreasing protein expression instead of only

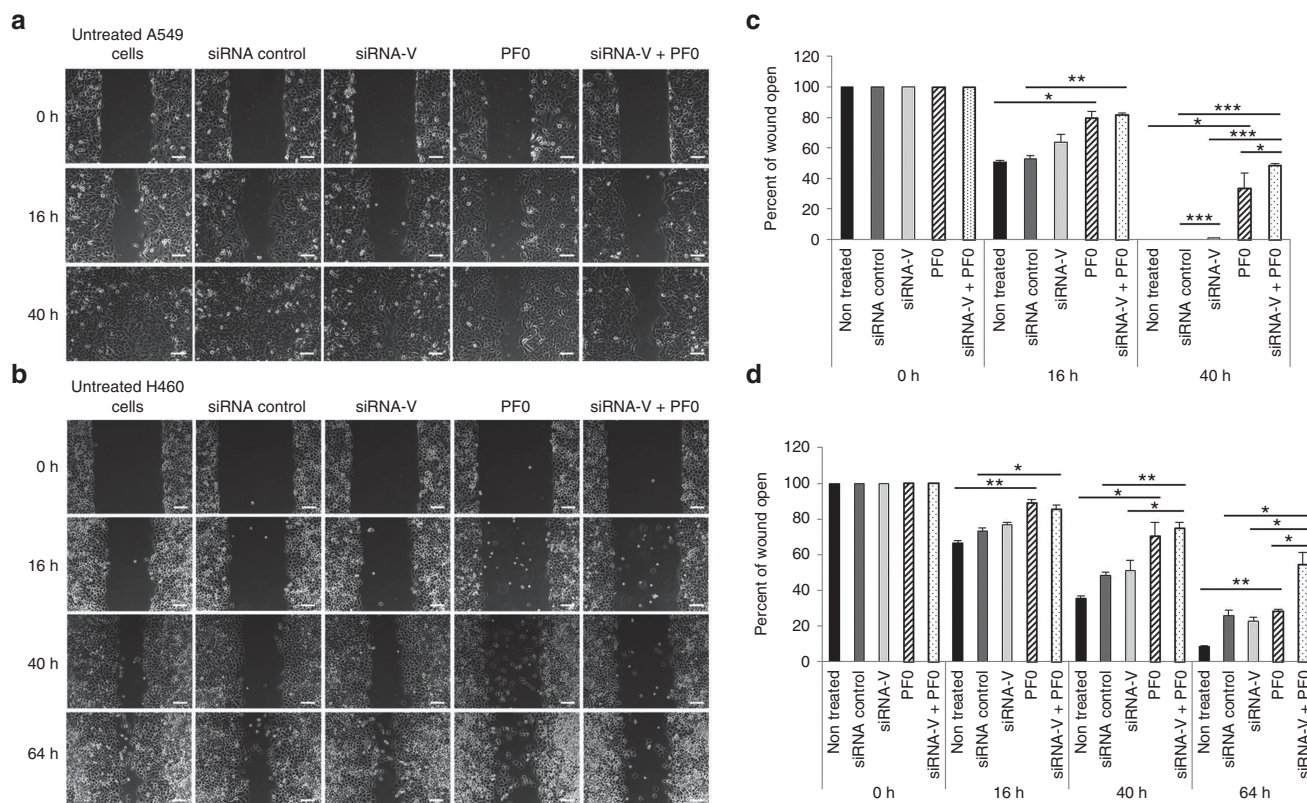


Figure 5 Inhibition of cell migration by siRNA-V and PF0. Representative micrographs of migrating treated and untreated (a) A549 and (b) H460 cells from three independent experiments are shown. The open image area was calculated for (c) A549 and (d) H460 experiments using TScratch program, reflecting the degree of migration or wound healing. Confluent monolayers of A549 and H460 cells were wounded, and the cells were allowed to migrate for 40 and 64 hours respectively in the presence or absence of drugs. Wound space was visualized under a phase contrast microscope and analyzed by comparing the relative change in wound space of the treated over nontreated cell mono-layers. Values were given as mean value \pm standard deviation of three independent experiments. Asterisks indicate statistical significance (* $P < 0.05$, ** $P < 0.01$, *** $P < 0.001$). Scale bar = 100 μ m.

sequestering the protein.¹⁶ Gene therapy utilizing siRNA to target *VEGF* has demonstrated promising *in vitro* and *in vivo* antitumor activity against variety of cancers,^{18,19} and its effect may be further improved in combination with other anticancer agents.

The PI3K/mTOR signaling cascade is one of the most frequently disrupted in human cancer leading to tumor progression and development and FDA-approved drugs are available to inhibit this pathway.^{21,37} Efforts are now placed in novel compounds capable of inhibiting both PI3K and mTOR, completely shutting down the PI3K/Akt/mTOR pathway.^{38,39} These small molecules block both mTORC1-dependent phosphorylation of p70S6K and mTORC2-dependent phosphorylation of Akt overcoming feedback loops⁴⁰ (Figure 1a). PI3K/mTOR dual inhibitors have shown promising results in preclinical and clinical studies^{26,27} and some of these agents are now entering phase 2 clinical trials.²²

Our study explores a unique approach that targets three proteins and two important pathways for lung cancer survival and angiogenesis. In the current study we demonstrated for the first time that PF0 and siRNA-V combination leads to an enhanced anticancer activity against non-small-cell lung cancer cells. We first performed a dose-response study for PF0 and siRNA-V to evaluate the *in vitro* cytotoxicity effect in NSCLC cells. Previous results had shown that PF0 effectively

inhibited tumor cell proliferation and showed antitumor efficacy in NSCLC xenograft models.²⁸ Our results showed a dose- and time-dependent cytotoxicity of PF0 in both cell lines, with lower IC₅₀ values in A549 (151.45 to 209.77 nmol/l) than in H460 cells (936.7 to 1965.5 nmol/l) (Figure 1b,d and Supplementary Figures S1a and S2a). Our study indicates that H460 cells require higher concentrations of PF0 to produce anticancer activity compared with A549 suggesting that H460 cells are less sensitive to PF0 treatment. Therefore, it is possible that H460 cells may be using multiple pathways for survival downstream of PI3K whereas A549 predominantly use the PI3K/mTOR pathway. The antitumor effect of PI3K/mTOR dual inhibitors vary significantly among cancer types, including cell lines,^{28,41} which might relate to the complexity of the signaling networks. Previous studies reported highly different IC₅₀ values to PF0 (0.1 to 2 μ mol/l) in a wide panel of head and neck carcinoma cell lines suggesting that different factors contribute to the sensitivity of cancer cells to the drug.⁴²

siRNA-V cytotoxicity analysis showed a dose-dependent antiproliferative effect against A549 and H460 cells (Figure 1c,e and Supplementary Figures S1b and S2b). Our results showed the highest effect of siRNA-V at 72 hours with IC₅₀ values of approximately 60 nmol/l for A549 and 40 nmol/l for H460 cells. siRNA-V treatment showed a higher

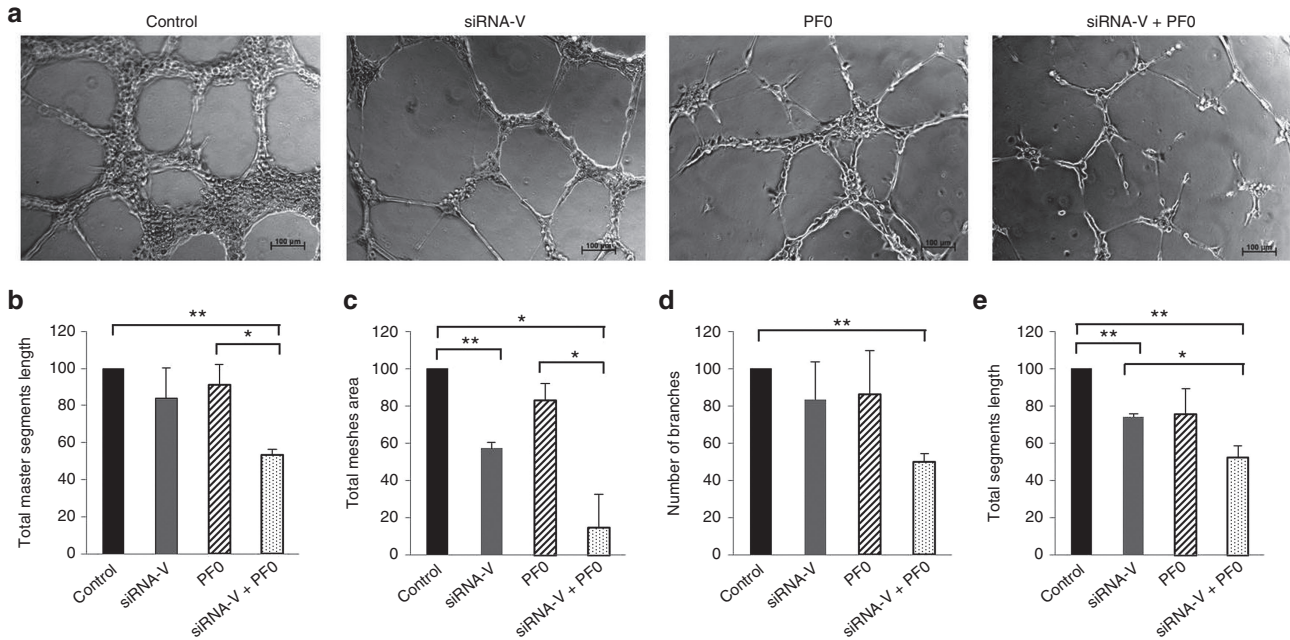


Figure 6 Antiangiogenic effect of siRNA-V and PF0. (a) Representative images of the human umbilical vein endothelial cells (HUVEC) tube formation assay after 6 hours treatment. Quantification of (b) total master segments length, (c) total meshes area, (d) number of branches, and (e) total segments length. HUVEC cells were transfected with siRNA-V (50 nmol/l), treated with PF0 (100 nmol/l) single drugs and combination on polymerized Matrigel at 37 °C. After 6 hours, tube formation by endothelial cells was photographed and quantified with the angiogenesis analyzer from ImageJ 1.49 software. Control cells were scramble siRNA treated cells. Data are expressed as mean ± standard deviation of three independent experiments. Asterisks indicate statistical significance (* $P < 0.05$, ** $P < 0.01$, *** $P < 0.001$). Scale bar = 100 μ m.

Table 1 Combination treatment of PF0 and siRNA-V in A549 and H460 cells for 72 hours

| Lung cancer cell line | Concentration, IC ₅₀ equivalent | | Combination index at 50% effect level | Evaluation at 50% effect level | IC ₅₀ PF0 | IC ₅₀ siRNA-V |
|-----------------------|--|---------|---------------------------------------|--------------------------------|----------------------|--------------------------|
| | PF0 | siRNA-V | | | | |
| A549 | 0.52 | 0.10 | 0.62 | Moderate synergism | 139.10 | 6.00 |
| | 0.51 | 0.20 | 0.71 | Moderate synergism | 134.15 | 12.00 |
| | 0.58 | 0.30 | 0.88 | Slight synergism | 152.15 | 18.00 |
| H460 | 0.66 | 0.10 | 0.76 | Moderate synergism | 610.05 | 4.00 |
| | 0.31 | 0.20 | 0.51 | Synergism | 281.90 | 8.00 |
| | 0.51 | 0.30 | 0.81 | Slight synergism | 470.00 | 12.00 |

The concentration in IC₅₀ equivalent of PF0 was calculated by dividing the IC₅₀ of PF0 in combination with siRNA-V from its corresponding single-agent IC₅₀ value (IC₅₀ of the combination/PF0 IC₅₀). For siRNA-V, the concentration in IC₅₀ equivalent was calculated by dividing its actual concentration used in the combination treatment from its corresponding single-agent IC₅₀ value (siRNA-V/siRNA-V IC₅₀). Combination index (CI) at 50% effect level is calculated by adding the IC₅₀ equivalent concentration of PF0 and siRNA-V. CI > 1.1 is antagonism; CI = 0.9–1.1 is additive; CI = 0.8–0.9 is slight synergism; CI = 0.6–0.8 is moderate synergism; CI = 0.4–0.6 is synergism; CI = 0.2–0.4 is strong synergism. The data present the average of three independent experiments performed in triplicate (n = 9).

inhibition of H460 survival as compared to A549 suggesting that H460 cells are more sensitive to siRNA-V treatment. After 72 hours of siRNA-V treatment, cell viability was decreased 27% in A549 cells (Figure 1c) and 42% in H460 cells (Figure 1e). Previous reports had shown that VEGF stimulates tumor cell proliferation in NSCLC^{43,44} and siRNA-V treatment resulted in tumor suppression in lung cancer animal models.⁴⁵

The analysis of different combinations of PF0 and siRNA-V demonstrated an enhanced therapeutic cytotoxicity against NSCLC. The combination treatment showed a significantly ($P < 0.05$) higher effect reducing cell survival compared to single-agent therapy after 24, 48, and 72 hours (Figure 2a,b). Therefore, this combination therapy could potentially be more effective and have fewer side effects than either agent alone,

thereby providing a rationale for combining these drugs as a treatment for NSCLC.

To ensure optimal siRNA-V transfection efficiency and evaluate the effect on VEGF expression, we analyzed mRNA and protein expression levels. Our real-time PCR results showed a significant ($P < 0.05$) decrease in VEGF expression after 48 hours treatment with siRNA-V or siRNA-V + PF0 in A549 and H460 cells (Figure 3a,b). Furthermore, an ELISA showed that secreted human VEGF levels were significantly ($P < 0.05$) reduced in A549 and H460 cells after 24–72 hours siRNA-V transfection and after PF0 treatment as compared with controls (Figure 3c,d). As predicted, PI3K/mTOR inhibitors can decrease VEGF secretion and angiogenesis.⁴⁶ Activation of the PI3K/Akt pathway in tumor cells can increase VEGF secretion, both by HIF1 α -dependent

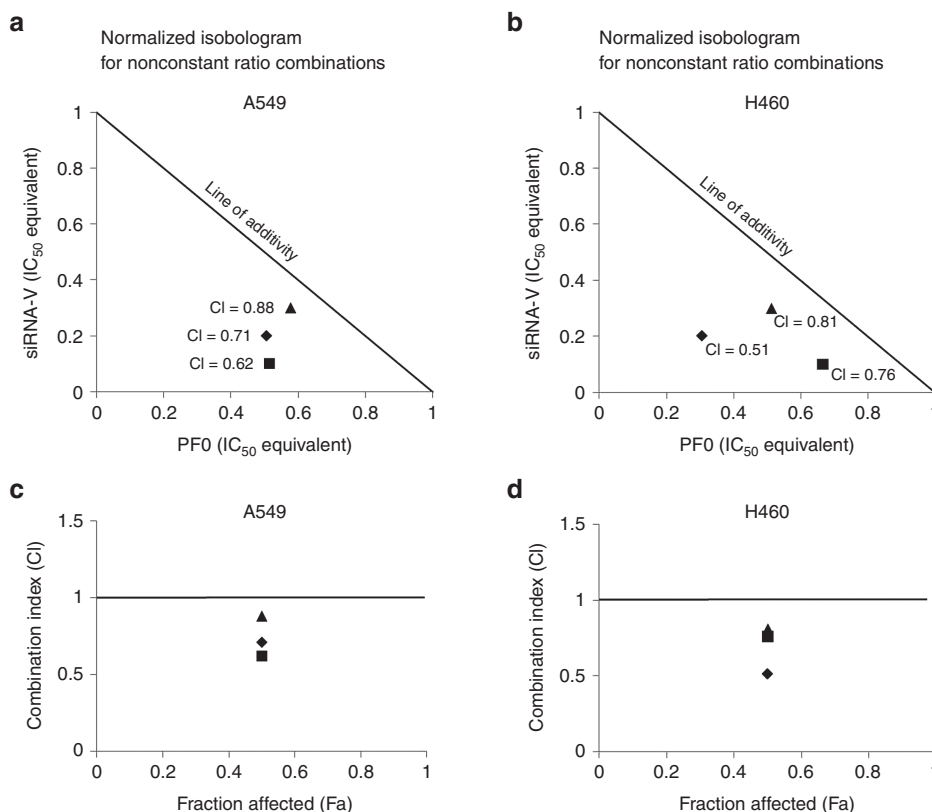


Figure 7 Normalized isobologram for nonconstant ratio combination design of siRNA-V and PF0. Isobologram analysis was performed to determine the cytotoxicity of siRNA-V and PF0 combination against (a) A549 and (b) H460 lung cancer cells. The half maximal inhibitory concentration (IC₅₀) of the combinations was determined after 72 hours of treatment. The siRNA-V dose was fixed to 6, 12, and 18 nmol/l for A549, and 4, 8, and 12 nmol/l for H460 cells, corresponding to 0.1 (■), 0.2 (◆), and 0.3 (▲) IC₅₀ equivalents respectively. The concentration in IC₅₀ equivalent for siRNA-V was calculated by dividing its actual concentration used in the combination treatment from its corresponding single-agent IC₅₀ value. Different concentrations of PF0 (5 nmol/l to 5 μmol/l for A549, and 5 nmol/l to 100 μmol/l for H460 cells) were combined to the fixed doses of siRNA-V. The concentration in IC₅₀ equivalent of PF0 was calculated by dividing the IC₅₀ of PF0 in combination with siRNA-V from its corresponding single-agent IC₅₀ value. CI at 50% effect level was calculated by adding the IC₅₀ equivalent concentration of PF0 and siRNA-V used in combination by using the CI equation. The line of additivity on the isobologram represents the 50% effect level of each drug. Synergy, additivity, or antagonism effects are indicated below, on, or above the line of additivity, respectively. CI > 1.1 is antagonism; CI = 0.9–1.1 is additivity; CI < 0.9 is synergy. Fraction affected vs. combination index (Fa-CI) plot was generated for A549 (c) and H460 (d) cell lines for the combination of siRNA-V and PF0 using a non-constant drug ratio. CI values were calculated for each experiment at 0.5 Fa (indicating 50% of cells inhibited after drug exposure). CI values were calculated for a fixed dose of siRNA-V of 0.1 (■), 0.2 (◆), and 0.3 (▲) IC₅₀ equivalents (corresponding to 6, 12, and 18 nmol/l for A549, and 4, 8, and 12 nmol/l for H460 cells respectively). The data present the average of three independent experiments in triplicate ($n = 9$).

and -independent mechanisms.^{23,24} The combination treatment resulted in almost undetectable levels of secreted VEGF. The 72-hour combination treatment resulted in a significant ($P < 0.05$) decrease in VEGF expression compared with single-agent treatments suggesting that the combination is highly effective. Our western blot data showed that PF0 inhibits PI3K and mTOR pathways in NSCLC cells after 24–72 hours treatment. PF0 single agent and in combination with siRNA-V significantly ($P < 0.05$) inhibited the phosphorylation of Akt (S473), a PI3K and mTORC2 downstream target, in A549 and H460 cells (Figure 3e,f and Supplementary Figures S3 and S4). PF0 also significantly ($P < 0.05$) inhibited the phosphorylation of mTORC1 downstream target p70S6K (T389). The decrease in p-Akt/Akt and p-p70S6K/p70S6K ratio after PF0 treatment was significant ($P < 0.05$) at all the analyzed time points (24–72 hours) and as expected there was no change in total Akt and p70S6K levels (Figure 3e,f and Supplementary Figures

S3 and S4). Previous studies reported that short-term exposure to PF0 predominantly inhibited PI3K, whereas mTOR inhibition persisted for more than 48 hours.²⁸ Kinetic studies of PF0 and other PI3K/mTOR dual inhibitors had shown that levels of p-Akt (S473) and p-p70S6K (T389) decrease below control levels after 3 to 72 hours treatment.^{47–49} This is in agreement with our results showing that phosphorylation of Akt and p70S6K was significantly ($P < 0.05$) inhibited after 24–72 hours.

To investigate the long-term effect of PF0 and siRNA-V on proliferation of lung cancer cells, an anchorage dependent colony formation assay was performed (Figure 4a,b). Results showed a decreased number of colonies after siRNA-V or PF0 treatment. Previous publications reported long-term treatment with PF0 significantly suppressed the *in vitro* colony-forming abilities of cancer cells.^{50,51} siRNA targeting VEGF was also previously reported to be effective to significantly decrease cancer cell colony formation.⁵² The

combination resulted in a significant ($P < 0.05$) colony formation decrease when compared with single-agent treatment (Figure 4c,d). These results indicated that VEGF knock-down contributed to the suppressive effect of PF0 to a final enhanced effect of the combination therapy on lung cancer colony formation.

Cell migration is an integral part of metastasis that is required at virtually every step of the metastatic cascade.⁵³ Wound healing assays showed a significant ($P > 0.05$) effect of siRNA-V on A549 cell migration (Figure 5a,c). Previous reports showed that VEGF signaling can promote migration and invasion of cancer cells and siRNA treatment reduces the migration rates.^{52,54} PF0 treatment resulted in a significant ($P < 0.05$) decrease in cell migration in A549 and H460 cells, indicating that PI3K/mTOR pathway plays a central role in tumorigenesis by regulating migration of cancer cells, which is in agreement with previous reports.³⁷ Migration of both NSCLC cells after combination treatment was significantly ($P > 0.05$) decreased compared with single agents (after 40 hours treatment in A549 cells and 64 hours in H460 cells) (Figure 5). Herein, we provided evidence of the siRNA-V and PF0 combination efficacy to inhibit lung cancer cell migration.

To study the possible mechanism involved in the enhanced cytotoxicity of siRNA-V and PF0, we evaluated the antiangiogenic effect in HUVEC tube formation. This assay is critical for evaluating drug antiangiogenic activity *in vitro*. Tube formation assays are considered representative of the later stages of angiogenesis and they are used as a model of *in vivo* capillary development.⁵⁵ The siRNA-V (50 nmol/l) treatment showed a significant ($P < 0.01$) decrease in total meshes area and segments length compared to control, which showed a rich meshwork of branching anastomosing capillary-like tubules with multicentric junctions (Figure 6a,c,e). It is already known that VEGF stimulates endothelial branching morphogenesis.⁵⁶ Previous reports showed that VEGF enhanced the ability of HUVEC to organize into tubular networks on Matrigel⁵⁷ and that tube formation is reduced by VEGF inhibitors or siRNA.^{58,59} PF0 (100 nmol/l) treatment showed a nonsignificant ($P < 0.05$) decrease in tube segments length compared to control (Figure 6a,e). Previous studies showed that higher concentrations of PI3K/mTOR dual inhibitors (1 $\mu\text{mol/l}$) significantly ($P > 0.05$) decreased HUVEC tube formation and tumor angiogenesis.⁶⁰ siRNA-V and PF0 combination showed the linear structures of the network were clearly disrupted compared to single-agent treatment (Figure 6a) presenting a significant ($P < 0.05$) decrease of the total segment length or total meshes area (Figure 6c,e). Compounds that are able to inhibit tube formation are very useful in cancer treatment, where tumors stimulate new blood vessel formation to grow beyond a relatively small size.¹²

CI analyses, isobologram, and Fa-CI plots were used to test whether the PF0 and siRNA-V combination treatment induces synergistic cell death in NSCLC (Figure 7). We calculated the CIs using the Chou-Talalay method⁶¹ by combining siRNA-V (0.1–0.3 IC_{50} equivalents) and PF0 (0.5–5 $\mu\text{mol/l}$ for A549, and 0.5–100 $\mu\text{mol/l}$ for H460 cells) treatments for 72 hours. The CIs ranged from 0.51 to 0.88 in A549 and H460 cell lines (Table 1), suggesting that the synergistic effect was induced in both adenocarcinoma and large cell carcinoma

NSCLC cells. This synergistic effect was contributed due to targeting of multiple proteins: VEGF, PI3K, and mTOR.⁴⁰ Therefore, the use of this combination will be beneficial for lung cancer treatment.

Conclusion

Our results revealed the synergistic interaction between VEGF and PI3K/mTOR signaling in NSCLC cell proliferation, which suggest a promising therapeutic benefit of PF0 and siRNA-V combination for NSCLC treatment. The developed combination therapy also showed a decrease in long-term proliferation in A459 and H460 colony formation assays. *In vitro* wound healing assay showed a decrease in cell migration after siRNA-V and PF0 treatment. The combination therapy also showed an enhanced effect decreasing progression of angiogenesis and tube formation organization. Overall, our results suggest that the developed combination therapy, which preferentially targets tumor proliferation, migration, and angiogenesis, may be effective for the treatment of lung solid tumors and other types of cancers. However, further preclinical studies are warranted to evaluate the anticancer activity of PF0 and siRNA-V combination. Our ongoing combination studies are focused on the use of biocompatible targeted nanoparticles to effectively codeliver siRNA-V and PF0 to NSCLC while sparing normal tissues.

Materials and methods

Cell culture and treatment. We have selected human slow growing A549 adenocarcinoma cells and fast growing H460 large-cell carcinoma cells to evaluate the anticancer effect based on our previous studies.^{30,31} The A549 and H460 NSCLC cells were obtained from American Type Culture Collection (Rockville, MD). A549 and H460 cells were grown in F12K and RPMI 1640 medium (Sigma Aldrich, St. Louis, MO) supplemented with 10% fetal bovine serum respectively. Pooled donor HUVEC cells (Lonza, Portsmouth, NH) were cultured in EGM BulletKit medium (Lonza) supplemented with 10% fetal bovine serum. All tissue culture media contained antibiotic antimycotic solution of penicillin (5,000 U/ml), streptomycin (0.1 mg/ml), and neomycin (0.2 mg/ml). All cells were grown at 37 ± 0.5 °C in a humidified 95% air and 5% CO_2 atmosphere.

Gene knockdown was achieved using SMART pool ON-TARGETplus siRNA (Dharmacon, Boston, MA) targeting human VEGF. Target RNA sequences: 5'-GCAGAAUCAUCAG AAGUG-3', 5'-CAACAAAUGUGAAUUGCAGA-3', 5'-GGAGUA CCCUGAUGAGAUC-3', 5'-GAUCAAAACCACCAAGGC-3'. ON-TARGETplus Non-targeting Pool was used as negative control. Target RNA sequences: 5'-UGGUUUACAUGUCGA CUAA-3', 5'-UGGUUUACAUGUUGUGUGA-3', 5'-UGGUUU ACAUGUUUUCUGA-3', 5'-UGGUUUACAUGUUUCCUA-3'. Transfection was performed using DharmaFECT 1 transfection reagent (Dharmacon) in Opti-MEM I reduced serum medium (Thermo Fisher Scientific, Waltham, MA) without antibiotics and following the manufacturer's instructions. PF-04691502 was purchased from Abmole Bioscience (Houston, TX). PF0 was first dissolved in dimethyl sulfoxide

to a final dilution of 10 mmol/l and then diluted in the appropriate aqueous culture medium.

In vitro cytotoxicity studies. For the cytotoxicity studies, A549 or H460 cells were plated in 96-well flat-bottomed tissue culture plates, at a density of 5×10^3 and 6×10^3 cells/well respectively and were allowed to incubate overnight. To evaluate the dose–response effect to the siRNA the cells were transfected with different concentrations of siRNA-V (5 to 150 nmol/l for A549, 5 to 200 nmol/l for H460) and DharmaFECT 1 reagent. To evaluate the dose–response effect to PF0 the cells were treated with various dilutions of PF0 (5 to 5,000 nmol/l in A549 and 5 nmol/l to 200 μ mol/l in H460 cells). The IC_{50} values of siRNA-V and PF0 for A549 and H460 cell lines were calculated using the nonlinear log inhibitor versus normalized response curve fit function from GraphPad PRISM 3.0 software (San Diego, CA).

To analyze the effect of the combination, the cells were treated with various dilutions of PF0 (5 to 500 nmol/l for A549, 10 to 5,000 nmol/l for H460) in the presence of siRNA-V (50 nmol/l) as described previously.³⁰ The PF0 concentrations for the combination studies were selected based on the previous single-agent cytotoxicity results. 50 nmol/l siRNA-V concentration was selected for the transient transfection of the cells to obtain a high transfection efficiency. The plates were incubated for 24, 48, or 72 hours in a humidified atmosphere of 5% CO_2 at 37 ± 0.5 °C. Cell viability in each treatment group was determined by resazurin (Sigma Aldrich) dye assay. Briefly, 15 μ l of resazurin (0.1 mg/ml) in PBS (pH 7.4) were mixed with 85 μ l of culture medium and the total 100 μ l were added to each well. The plate was incubated for 3 hours at 37 ± 0.5 °C. The absorbance was measured at 550/580 nm using a microplate reader (BioTek, Winooski, VT).

Combination index analysis, normalized isobologram, and Fa-CI plot. A quantitative assessment of non-constant ratio combinations (fixed-dose combinations) of siRNA-V and PF0 was carried out *in vitro* to measure the drugs' interaction at 50% effect level. Excel software was used to plot a normalized isobologram and Chou-Talalay method⁶¹ was used to determine the CI values, which express pharmacologic drug interactions, for each cell line combination treatment. Based on the single-agent IC_{50} determination, each NSCLC cell line was treated for 72 hours with a combination of siRNA-V and PF0 at different concentrations. We fixed the concentration of siRNA-V to 6, 12, and 18 nmol/l for A549, and 4, 8, and 12 nmol/l for H460 cells, corresponding to 0.1, 0.2, and 0.3 IC_{50} equivalents respectively. The concentration in IC_{50} equivalent for siRNA-V was calculated by dividing its actual concentration used in the combination treatment from its corresponding single-agent IC_{50} value. PF0 concentrations ranging from 5 nmol/l to 5 μ mol/l, and 5 nmol/l to 100 μ mol/l were used to treat A549 and H460 cells, respectively. The concentration in IC_{50} equivalent of PF0 was calculated by dividing the IC_{50} of PF0 in combination with siRNA-V from its corresponding single-agent IC_{50} value. The CI values at 50% effect level were calculated using the CI equation by adding the values of the IC_{50} equivalents of siRNA-V and PF0 in combination with each other. The line of additivity on the isobologram represents the 50% effect level of each drug. $CI > 1.1$ is antagonism; $CI = 0.9–1.1$ is additive;

$CI = 0.8–0.9$ is slight synergism; $CI = 0.6–0.8$ is moderate synergism; $CI = 0.4–0.6$ is synergism; $CI = 0.2–0.4$ is strong synergism. The experiment was performed three independent times in triplicate ($n = 9$). Fa-CI plot was also generated for A549 and H460 cell lines for the combination of siRNA-V and PF0 using a non-constant drug ratio. CI values were calculated for each experiment at 0.5 Fa, indicating 50% of cells inhibited after drug exposure.

Quantitative real-time PCR. A549 and H460 cells ($2 \times 10^5/2.4 \times 10^5$) in six-well plates were allowed to incubate overnight and after that were treated with siRNA-V and PF0 combination and single agents. The PF0 and siRNA-V concentrations for the expression analysis and the following colony formation and wound healing assays were selected based on the previous single-agent cytotoxicity results and the observed IC_{50} values for each cell line. The selected PF0 concentration for A549 treatment was 200 nmol/l (IC_{50} values 151.45 to 209.77 nmol/l between 24 and 72 hours treatment), and the selected concentration for H460 treatment was 2,000 nmol/l (IC_{50} values 936.7 to 1,965.5 nmol/l). For the transient transfection of A549 and H460 cells 50 nmol/l siRNA-V concentration was selected (IC_{50} values 19.04 to 58.89 nmol/l in A549 and 26.19 to 40.79 nmol/l in H460 cells between 24 and 72 hours treatment) to ensure a high transfection efficiency. Total RNA was isolated 48 hours after treatment using High Pure RNA Isolation Kit (Roche, Indianapolis, IN). mRNA was reverse transcribed to cDNA using iScript Reverse Transcription Supermix (Bio-Rad, Hercules, CA). Gene levels were measured by iQ SYBR Green Supermix (Bio-Rad) and CFX384 Touch Real-Time PCR Detection System (Bio-Rad). Predesigned primers (KiCqStart SYBR Green Primers) for gene expression analysis of *VEGF* and *GAPDH* were purchased from Sigma Aldrich. Data are shown as percentage in *VEGF* mRNA expression normalized with *GAPDH*. Experiments were repeated three times in triplicate, and Bio-Rad CFX Manager Software v3.1 was used for gene pool quantification and statistical analysis. Calculations were performed using the double delta Ct method.⁶²

ELISA. A549 and H460 cells ($5 \times 10^3/6 \times 10^3$ cells/well respectively) in 96-well plates were treated with siRNA-V + PF0 (50 and 200 nmol/l respectively for A549 and 50 and 2,000 nmol/l respectively for H460) and single agents for 24, 48, and 72 hours. Culture medium was collected and secreted VEGF was determined using human VEGF-A ELISA kit (Pierce biotechnology/Thermo Scientific, Rockford, IL) following manufacturer's instructions. Absorbance was measured on a microplate reader (BioTek) at 450 nm minus 550 nm. Inhibition of VEGF secretion was calculated using a standard curve.

Western blot analysis. A549 and H460 cells ($2 \times 10^5/2.4 \times 10^5$) in six-well plates were allowed to incubate overnight. After that cells were treated with siRNA-V (50 nmol/l) and PF0 (2,000 nmol/l for A549 and 2,000 nmol/l for H460) combination and single agents using the corresponding controls. After 24, 48, and 72 hours of incubation cells were lysed in radioimmunoprecipitation assay buffer (50 mmol/l Tris–HCl pH 7.40, 150 mmol/l NaCl, 2 mmol/l ethylenediaminetetraacetic acid, 1% NP-40, 0.1% sodium dodecyl sulfate) with freshly added

protease and phosphatase inhibitors (Sigma Aldrich). Equivalent amounts of protein (20 µg) were subjected to sodium dodecyl sulfate–polyacrylamide gel electrophoresis, followed by electroblotting onto nitrocellulose membrane. Relative protein expression levels of phospho-Akt (S473), Akt, phospho-p70S6K (T389), and p70S6K were determined by Western blot analysis and GAPDH served as a protein loading control. Membranes were immunoblotted with the indicated primary antibodies (all used at a 1:1,000 dilution) at 4 °C overnight. Horseradish peroxidase-conjugated anti-rabbit (1:2,000 dilution) secondary antibody (Santa Cruz Biotechnology, Santa Cruz, CA) was then added at room temperature for 1 hour, and protein signals on membranes were visualized by Clarity Western ECL Chemiluminescent Substrate (Bio-Rad). Primary antibodies used were from Cell Signaling (Danvers, MA) except anti-GAPDH from Santa Cruz Biotechnology.

Anchorage-dependent colony formation assay. Mono-layer colony formation assay was performed in the continuous presence of drug or siRNA. A549 and H460 cells were seeded in six-well culture plates ($5 \times 10^3/6 \times 10^3$) and anchorage-dependent clonogenicity assay was performed. Twenty-four hours after plating A549 and H460 cells were transfected with 50 nmol/l siRNA-V, using nontreated cells and scramble siRNA-treated cells as controls. After that the cells were treated with PF0 (200 nmol/l for A549 and 2,000 nmol/l for H460 cells), single agent and in combination with 50 nmol/l siRNA-V. Cells were maintained in culture for 10 days to let the viable cells propagate to sizable colonies for quantification. Since the drugs were not replenished in the medium, the colony formation is a stringent assessment of the drug effect after single exposure. The colonies were fixed with methanol-acetic acid at 3:1 ratio and stained with 1% crystal violet for 30 minutes at room temperature. The number of colonies formed in each well was photographed under a dissecting microscope Leica MZ10F (Leica Microsystems, Wetzlar, Germany) at 0.8× magnification and counted using the ColonyCounter plugin on ImageJ 1.49 software.

Cell migration wound healing assay. A549 and H460 cells ($2 \times 10^5/2.4 \times 10^5$) were seeded into six-well plates and after 24 hours were transfected with 50 nmol/l siRNA-V and the appropriate controls. After 6 hours and at approximately 80–90% confluency, the cells were treated with PF0 (200 nmol/l for A549 and 2,000 nmol/l for H460 cells) and appropriate controls. The wound of approximately 1 mm in width was scratched with a 200 µl pipette tip. Wound closure was monitored at different time intervals for the next 40 and 64 hours in A549 and H460 cells respectively and imaged with a Zeiss Axiovert 40 CFL inverted microscope (Carl Zeiss AG, Oberkochen, Germany) using 10× magnification. The open area (scratch) was quantified with TScratch software (ETH Zurich, Swiss).⁶³

Endothelial cell tube formation. The antiangiogenic effects of siRNA-V and PF0 single agents and combination were visualized analyzing *in vitro* inhibition of tube formation of HUVEC as described previously.³¹ HUVEC were cultured in the presence or absence of 50 nmol/l siRNA-V and 100 nmol/l PF0 alone or in combination for 6 hours on polymerized Matrigel at 37 °C.

Standard Matrigel was allowed to polymerize in 96-well plates and HUVEC were seeded at a density of 1.5×10^4 per well in EGM medium. After 6 hours treatment, endothelial cells were fixed and tube formation was evaluated and photographed in a Zeiss Axiovert 40 CFL inverted microscope (Carl Zeiss AG) using 10× magnification. Quantification of angiogenesis progression was accomplished using the angiogenesis analyzer from ImageJ 1.49 by counting the total master segments length, total meshes area, capillary tube branch points, and total segments formed after 6 hours (end-point assay).

Statistical analysis. The experiments were repeated three times and the resulting data are presented after statistical processing. Data from multiple independent experiments are expressed as mean ± standard deviation. One-way analysis of variance followed by Tukey's Multiple Comparison Test was performed to determine the significance of differences among groups using GraphPad PRISM 3.0 software (San Diego). Differences were considered statistically significant at $P < 0.05$ in all experiments. * $P < 0.05$, ** $P < 0.01$, *** $P < 0.001$.

Supplementary material

Figure S1. Cytotoxicity effect of PF0 or siRNA-V in A549 cells after 24 and 48 hours treatment.

Figure S2. Cytotoxicity effect of PF0 or siRNA-V in H460 cells after 24 and 48 hours treatment.

Figure S3. Densitometric analysis of the Western blots presented in figure 4e (A549 cells) was carried out using Image J software.

Figure S4. Densitometric analysis of the Western blots presented in figure 4f (H460 cells) was carried out using Image J software.

Acknowledgments The authors acknowledge the support of the National Institute of General Medical Science of the National Institutes of Health under award number SC3GM109873. Authors acknowledge Hawai'i Community Foundation, Honolulu, HI 96813, USA, for research support on lung cancer (LEAHI FUND for Pulmonary Research Award; ID# 15ADVC-74296). We acknowledge the 2013 George F. Straub Trust and Robert C. Perry Fund of the Hawai'i Community Foundation, Honolulu, HI 96813, USA, for research support on lung cancer. The authors acknowledge the Department of Pharmaceutics and Drug Delivery, School of Pharmacy, University of Mississippi, University, MS, USA for providing start-up support to Dr. Chougule's lab. The authors also acknowledge a seed grant from the Research Corporation of the University of Hawai'i at Hilo, Hilo, HI 96720, USA, and The Daniel K. Inouye College of Pharmacy, University of Hawaii at Hilo, Hilo, HI 96720, USA, for providing start-up financial support to their research group. We thank Patrick John Sinko (Ernest Mario School of Pharmacy, Rutgers University, New Jersey) for his input on evaluation of combination therapy. Authors thank Rakesh Tekade (School of Pharmacy, International Medical University, Kuala Lumpur, Malaysia) for his initial inputs on the selection of PF0 and combination therapy.

1. American Cancer Society. <http://www.cancer.org/cancer/lungcancer-non-smallcell/detailedguide/non-small-cell-lung-cancer-survival-rates>.
2. Sheth, S (2010). Current and emerging therapies for patients with advanced non-small-cell lung cancer. *Am J Health Syst Pharm* **67**(1 Suppl 1): S9–14.
3. Amaraseena, IU, Walters, JA, Wood-Baker, R and Fong, K (2008). Platinum versus non-platinum chemotherapy regimens for small cell lung cancer. *Cochrane Database Syst Rev*: CD006849.
4. Carnio, S, Novello, S, Bironzo, P and Scagliotti, GV (2014). Moving from histological subtyping to molecular characterization: new treatment opportunities in advanced non-small-cell lung cancer. *Expert Rev Anticancer Ther* **14**: 1495–1513.
5. Cascone, T, Gridelli, C and Ciardiello, F (2007). Combined targeted therapies in non-small cell lung cancer: a winner strategy? *Curr Opin Oncol* **19**: 98–102.
6. Hanahan, D and Weinberg, RA (2011). Hallmarks of cancer: the next generation. *Cell* **144**: 646–674.
7. Schmid-Bindert, G (2013). Update on antiangiogenic treatment of advanced non-small cell lung cancer (NSCLC). *Target Oncol* **8**: 15–26.
8. Ellis, LM and Hicklin, DJ (2008). VEGF-targeted therapy: mechanisms of anti-tumour activity. *Nat Rev Cancer* **8**: 579–591.
9. Ferrara, N, Gerber, HP and LeCouter, J (2003). The biology of VEGF and its receptors. *Nat Med* **9**: 669–676.
10. Carrillo de Santa Pau, E, Arias, FC, Caso Pelaez, E, Munoz Molina, GM, Sanchez Hernandez, I, Muguuruza Trueba, I *et al.* (2009). Prognostic significance of the expression of vascular endothelial growth factors A, B, C, and D and their receptors R1, R2, and R3 in patients with nonsmall cell lung cancer. *Cancer* **115**: 1701–1712.
11. Han, H, Silverman, JF, Santucci, TS, Macherey, RS, d'Amato, TA, Tung, MY *et al.* (2001). Vascular endothelial growth factor expression in stage I non-small cell lung cancer correlates with neoangiogenesis and a poor prognosis. *Ann Surg Oncol* **8**: 72–79.
12. Hall, RD, Le, TM, Haggstrom, DE and Gentzler, RD (2015). Angiogenesis inhibition as a therapeutic strategy in non-small cell lung cancer (NSCLC). *Transl Lung Cancer Res* **4**: 515–523.
13. Sandler, A, Gray, R, Perry, MC, Brahmer, J, Schiller, JH, Dowlati, A *et al.* (2006). Paclitaxel-carboplatin alone or with bevacizumab for non-small-cell lung cancer. *N Engl J Med* **355**: 2542–2550.
14. Dempke, WC, Suto, T and Reck, M (2010). Targeted therapies for non-small cell lung cancer. *Lung Cancer* **67**: 257–274.
15. Chames, P, Van Regenmortel, M, Weiss, E and Baty, D (2009). Therapeutic antibodies: successes, limitations and hopes for the future. *Br J Pharmacol* **157**: 220–233.
16. Ozcan, G, Ozpolat, B, Coleman, RL, Sood, AK and Lopez-Berestein, G (2015). Preclinical and clinical development of siRNA-based therapeutics. *Adv Drug Deliv Rev* **87**: 108–119.
17. Garba, AO and Mousa, SA (2010). Bevasiranib for the treatment of wet, age-related macular degeneration. *Ophthalmol Eye Dis* **2**: 75–83.
18. Salva, E, Kabasakal, L, Eren, F, Ozkan, N, Cakalagaoglu, F and Akbuğa, J (2012). Local delivery of chitosan/VEGF siRNA nanoplexes reduces angiogenesis and growth of breast cancer *in vivo*. *Nucleic Acid Ther* **22**: 40–48.
19. Zhang, Y, Schwerbrock, NM, Rogers, AB, Kim, WY and Huang, L (2013). Codelivery of VEGF siRNA and gemcitabine monophosphate in a single nanoparticle formulation for effective treatment of NSCLC. *Mol Ther* **21**: 1559–1569.
20. Engelman, JA, Luo, J and Cantley, LC (2006). The evolution of phosphatidylinositol 3-kinases as regulators of growth and metabolism. *Nat Rev Genet* **7**: 606–619.
21. Courtney, KD, Corcoran, RB and Engelman, JA (2010). The PI3K pathway as drug target in human cancer. *J Clin Oncol* **28**: 1075–1083.
22. Fumarola, C, Bonelli, M, Petronini, PG and Alfieri, RR (2014). Targeting PI3K/AKT/mTOR pathway in non small cell lung cancer. *Biochem Pharmacol* **90**: 197–207.
23. Maity, A, Pore, N, Lee, J, Solomon, D and O'Rourke, DM (2000). Epidermal growth factor receptor transcriptionally up-regulates vascular endothelial growth factor expression in human glioblastoma cells via a pathway involving phosphatidylinositol 3'-kinase and distinct from that induced by hypoxia. *Cancer Res* **60**: 5879–5886.
24. Zhong, H, Chiles, K, Feldser, D, Laughner, E, Hanrahan, C, Georgescu, MM *et al.* (2000). Modulation of hypoxia-inducible factor 1alpha expression by the epidermal growth factor/phosphatidylinositol 3-kinase/PTEN/AKT/FRAP pathway in human prostate cancer cells: implications for tumor angiogenesis and therapeutics. *Cancer Res* **60**: 1541–1545.
25. Serra, V, Markman, B, Scaltriti, M, Eichhorn, PJ, Valero, V, Guzman, M *et al.* (2008). NVP-BE2235, a dual PI3K/mTOR inhibitor, prevents PI3K signaling and inhibits the growth of cancer cells with activating PI3K mutations. *Cancer Res* **68**: 8022–8030.
26. Cerniglia, GJ, Karar, J, Tyagi, S, Christofidou-Solomidou, M, Rengan, R, Koumenis, C *et al.* (2012). Inhibition of autophagy as a strategy to augment radiosensitization by the dual phosphatidylinositol 3-kinase/mammalian target of rapamycin inhibitor NVP-BE2235. *Mol Pharmacol* **82**: 1230–1240.
27. Kuger, S, Graus, D, Brendtke, R, Günther, N, Katzer, A, Lutjy, P *et al.* (2013). Radiosensitization of glioblastoma cell lines by the dual PI3K and mTOR inhibitor NVP-BE2235 depends on drug-irradiation schedule. *Transl Oncol* **6**: 169–179.
28. Yuan, J, Mehta, PP, Yin, MJ, Sun, S, Zou, A, Chen, J *et al.* (2011). PF-04691502, a potent and selective oral inhibitor of PI3K and mTOR kinases with antitumor activity. *Mol Cancer Ther* **10**: 2189–2199.
29. Minguet, J, Smith, KH and Bramlage, P (2016). Targeted therapies for treatment of non-small cell lung cancer—Recent advances and future perspectives. *Int J Cancer* **138**: 2549–2561.
30. Chougule, M, Patel, AR, Sachdeva, P, Jackson, T and Singh, M (2011). Anticancer activity of Noscapine, an opioid alkaloid in combination with Cisplatin in human non-small cell lung cancer. *Lung Cancer* **71**: 271–282.
31. Chougule, MB, Patel, A, Sachdeva, P, Jackson, T and Singh, M (2011). Enhanced anticancer activity of gemcitabine in combination with noscapine via antiangiogenic and apoptotic pathway against non-small cell lung cancer. *PLoS One* **6**: e27394.
32. Ichite, N, Chougule, MB, Jackson, T, Fulzele, SV, Safe, S and Singh, M (2009). Enhancement of docetaxel anticancer activity by a novel diindolylmethane compound in human non-small cell lung cancer. *Clin Cancer Res* **15**: 543–552.
33. Cook, KM and Figg, WD (2010). Angiogenesis inhibitors: current strategies and future prospects. *CA Cancer J Clin* **60**: 222–243.
34. Majeti, BK, Lee, JH, Simmons, BH and Shojaei, F (2013). VEGF is an important mediator of tumor angiogenesis in malignant lesions in a genetically engineered mouse model of lung adenocarcinoma. *BMC Cancer* **13**: 213.
35. Fontanini, G, Faviana, P, Lucchi, M, Boldrini, L, Mussi, A, Camacci, T *et al.* (2002). A high vascular count and overexpression of vascular endothelial growth factor are associated with unfavourable prognosis in operated small cell lung carcinoma. *Br J Cancer* **86**: 558–563.
36. Guo, W, Chen, W, Yu, W, Huang, W and Deng, W (2013). Small interfering RNA-based molecular therapy of cancers. *Chin J Cancer* **32**: 488–493.
37. Engelman, JA (2009). Targeting PI3K signalling in cancer: opportunities, challenges and limitations. *Nat Rev Cancer* **9**: 550–562.
38. Musa, F and Schneider R (2015). Targeting the PI3K/AKT/mTOR pathway in ovarian cancer. *Translational Cancer Research* **4**. No 1 (February 2015): Translational Cancer Research (Epithelial ovarian cancer treatment: integrating molecular targeting).
39. Dienstmann, R, Rodon, J, Serra, V and Tabernero, J (2014). Picking the point of inhibition: a comparative review of PI3K/AKT/mTOR pathway inhibitors. *Mol Cancer Ther* **13**: 1021–1031.
40. Pópulo, H, Lopes, JM and Soares, P (2012). The mTOR signalling pathway in human cancer. *Int J Mol Sci* **13**: 1886–1918.
41. Barretina, J, Caponigro, G, Stransky, N, Venkatesan, K, Margolin, AA, Kim, S *et al.* (2012). The Cancer Cell Line Encyclopedia enables predictive modelling of anticancer drug sensitivity. *Nature* **483**: 603–607.
42. Herzog, A, Bian, Y, Vander Broek, R, Hall, B, Coupar, J, Cheng, H *et al.* (2013). PI3K/mTOR inhibitor PF-04691502 antitumor activity is enhanced with induction of wild-type TP53 in human xenograft and murine knockout models of head and neck cancer. *Clin Cancer Res* **19**: 3808–3819.
43. Devery, AM, Wadekar, R, Bokobza, SM, Weber, AM, Jiang, Y and Ryan, AJ (2015). Vascular endothelial growth factor directly stimulates tumour cell proliferation in non-small cell lung cancer. *Int J Oncol* **47**: 849–856.
44. Mei, J, Gao, Y, Zhang, L, Cai, X, Qian, Z, Huang, H *et al.* (2008). VEGF-siRNA silencing induces apoptosis, inhibits proliferation and suppresses vasculogenic mimicry in osteosarcoma *in vitro*. *Exp Oncol* **30**: 29–34.
45. Chen, Y, Gu, H, Zhang, DS, Li, F, Liu, T and Xia, W (2014). Highly effective inhibition of lung cancer growth and metastasis by systemic delivery of siRNA via multimodal mesoporous silica-based nanocarrier. *Biomaterials* **35**: 10058–10069.
46. Karar, J and Maity, A (2011). PI3K/AKT/mTOR pathway in angiogenesis. *Front Mol Neurosci* **4**: 51.
47. Fang, DD, Zhang, CC, Gu, Y, Jani, JP, Cao, J, Tsaparikos, K *et al.* (2013). Antitumor efficacy of the dual PI3K/mTOR inhibitor PF-04691502 in a human xenograft tumor model derived from colorectal cancer stem cells harboring a PIK3CA mutation. *PLoS One* **8**: e67258.
48. Babichev, Y, Kabaroff, L, Datti, A, Uehling, D, Isaac, M, Al-Awar, R *et al.* (2016). PI3K/AKT/mTOR inhibition in combination with doxorubicin is an effective therapy for leiomyosarcoma. *J Transl Med* **14**: 67.
49. Wander, SA, Zhao, D, Besser, AH, Hong, F, Wei, J, Ince, TA *et al.* (2013). PI3K/mTOR inhibition can impair tumor invasion and metastasis *in vivo* despite a lack of antiproliferative action *in vitro*: implications for targeted therapy. *Breast Cancer Res Treat* **138**: 369–381.
50. Wang, FZ, Peng-Jiao, Yang, NN, Chuang-Yuan, Zhao, YL, Liu, QQ *et al.* (2013). PF-04691502 triggers cell cycle arrest, apoptosis and inhibits the angiogenesis in hepatocellular carcinoma cells. *Toxicol Lett* **220**: 150–156.
51. Wong, CH, Loong, HH, Hui, CW, Lau, CP, Hui, EP, Ma, BB *et al.* (2013). Preclinical evaluation of the PI3K-mTOR dual inhibitor PF-04691502 as a novel therapeutic drug in nasopharyngeal carcinoma. *Invest New Drugs* **31**: 1399–1408.
52. Doan, CC, Le, LT, Hoang, SN, Do, SM and Le, DV (2014). Simultaneous silencing of VEGF and KSP by siRNA cocktail inhibits proliferation and induces apoptosis of hepatocellular carcinoma Hep3B cells. *Biol Res* **47**: 70.
53. Yamaguchi, H, Wyckoff, J and Condeelis, J (2005). Cell migration in tumors. *Curr Opin Cell Biol* **17**: 559–564.
54. Wey, JS, Fan, F, Gray, MJ, Bauer, TW, McCarty, MF, Somcio, R *et al.* (2005). Vascular endothelial growth factor receptor-1 promotes migration and invasion in pancreatic carcinoma cell lines. *Cancer* **104**: 427–438.
55. Staton, CA, Reed, MW and Brown, NJ (2009). A critical analysis of current *in vitro* and *in vivo* angiogenesis assays. *Int J Exp Pathol* **90**: 195–221.
56. Yang, S, Xin, X, Zlot, C, Ingle, G, Fuh, G, Li, B *et al.* (2001). Vascular endothelial cell growth factor-driven endothelial tube formation is mediated by vascular endothelial cell

- growth factor receptor-2, a kinase insert domain-containing receptor. *Arterioscler Thromb Vasc Biol* **21**: 1934–1940.
57. Xu, H, Czerwinski, P, Hortmann, M, Sohn, HY, Förstermann, U and Li, H (2008). Protein kinase C alpha promotes angiogenic activity of human endothelial cells via induction of vascular endothelial growth factor. *Cardiovasc Res* **78**: 349–355.
58. Lee, SJ, Lee, I, Lee, J, Park, C and Kang, WK (2014). Statins, 3-hydroxy-3-methylglutaryl coenzyme A reductase inhibitors, potentiate the anti-angiogenic effects of bevacizumab by suppressing angiopoietin2, BiP, and Hsp90 α in human colorectal cancer. *Br J Cancer* **111**: 497–505.
59. Raskopf, E, Vogt, A, Sauerbruch, T and Schmitz, V (2008). siRNA targeting VEGF inhibits hepatocellular carcinoma growth and tumor angiogenesis in vivo. *J Hepatol* **49**: 977–984.
60. Rosich, L, Monraveta, A, Xargay-Torrent, S, López-Guerra, M, Roldán, J, Aymerich, M *et al.* (2014). Dual PI3K/mTOR inhibition is required to effectively impair microenvironment survival signals in mantle cell lymphoma. *Oncotarget* **5**: 6788–6800.
61. Chou, TC and Talalay, P (1984). Quantitative analysis of dose-effect relationships: the combined effects of multiple drugs or enzyme inhibitors. *Adv Enzyme Regul* **22**: 27–55.
62. Livak, KJ and Schmittgen, TD (2001). Analysis of relative gene expression data using real-time quantitative PCR and the 2(-Delta Delta C(T)) Method. *Methods* **25**: 402–408.
63. Gebäck, T, Schulz, MM, Koumoutsakos, P and Detmar, M (2009). TScratch: a novel and simple software tool for automated analysis of monolayer wound healing assays. *Biotechniques* **46**: 265–274.



This work is licensed under a Creative Commons Attribution-NonCommercial-ShareAlike 4.0 International License. The images or other third party material in this article are included in the article's Creative Commons license, unless indicated otherwise in the credit line; if the material is not included under the Creative Commons license, users will need to obtain permission from the license holder to reproduce the material. To view a copy of this license, visit <http://creativecommons.org/licenses/by-nc-sa/4.0/>

© The Author(s)(2016)

Supplementary Information accompanies this paper on the Molecular Therapy–Nucleic Acids website (<http://www.nature.com/mtna>)